HHS Public Access

Author manuscript

Clin Neurophysiol. Author manuscript; available in PMC 2016 May 01.

Published in final edited form as:

Clin Neurophysiol. 2015 May ; 126(5): 987–996. doi:10.1016/j.clinph.2014.09.006.

Dynamics of Functional and Effective Connectivity Within Human Cortical Motor Control Networks

Joshua B. Ewen, MD[a,b], **Balaji M. Lakshmanan, MS**[a], **Mark Hallett, MD**[c], **Stewart H. Mostofsky, MD**[b,d,e], **Nathan E. Crone, MD**[b], and **Anna Korzeniewska, PhD**[b]

Balaji M. Lakshmanan: lakshmanan@kennedykrieger.org; Mark Hallett: hallettm@ninds.nih.gov; Stewart H. Mostofsky: mostofsky@kennedykrieger.org; Nathan E. Crone: ncrone@jhmi.edu; Anna Korzeniewska: akorzen@jhmi.edu

[a]Department of Neurology and Developmental Medicine, Kennedy Krieger Institute, 707 N. Broadway, Baltimore, MD 21205, USA

[b]Department of Neurology, Johns Hopkins University School of Medicine, 600 N. Wolfe Street, Baltimore, MD 21287, USA

[c]Human Motor Control Section, Medical Neurology Branch, National Institutes of Neurological Disorders and Stroke, National Institutes of Health, Building 10, Room 7D37, 10 Center Drive, MSC 1428, Bethesda, MD 20892-1428, USA

[d]Laboratory for Neurocognitive and Imaging Research, Kennedy Krieger Institute, 707 N. Broadway, Baltimore, MD 21205, USA

[e]Department of Psychiatry and Behavioral Sciences, Johns Hopkins University School of Medicine, 600 N. Wolfe Street, Baltimore, MD 21287, USA

Abstract

Objective—Praxis, the performance of complex motor gestures, is crucial to the development of motor and social/communicative capacities. Praxis relies on a network consisting of inferior parietal and premotor regions, particularly on the left, and is thought to require transformation of spatio-temporal representations (parietal) into movement sequences (premotor).

Method—We examined praxis network dynamics by measuring EEG effective connectivity while healthy subjects performed a praxis task.

Results—Propagation from parietal to frontal regions was not statistically greater on the left than the right. However, propagation from left parietal regions to all other regions was significantly greater during gesture preparation than execution. Moreover, during gesture preparation only, propagation from the left parietal region to bilateral frontal regions was greater than reciprocal

Corresponding Author: Joshua B. Ewen, MD, Department of Neurology and Developmental Medicine, Kennedy Krieger Institute, 707 N. Broadway,, Baltimore, MD 21205, USA, Tel: +1-443-923-9170, ewen@kennedykrieger.org.

Conflict of Interest Statement

None of the authors has potential conflicts of interest to be disclosed.

propagations to the left parietal region. This directional specificity was not observed for the right parietal region.

Conclusions—These findings represent direct electrophysiological evidence for directionally predominant propagation in left frontal-parietal networks during praxis behavior, which may reflect neural mechanisms by which representations in the human brain select appropriate motor sequences for subsequent execution.

Significance—In addition to bolstering the classic view of praxis network function, these results also demonstrate the relevance of additional information provided by directed connectivity measures.

Keywords

EEG; effective connectivity; efference copy; praxis

1. Introduction

Praxis refers to the performance of skilled, complex motor gestures and is not only an important human capability in its own right but is also an excellent model for studying the performance and development of other human skills (Mostofsky and Ewen, 2011). The networks responsible for praxis skill learning and execution are of scientific interest for a number of reasons. Lesions of the praxis network are associated with the clinical syndrome of acquired apraxia, which is a clinical disorder that has attracted significant research(Wheaton and Hallett, 2007). Moreover, the anatomy of praxis network is relatively well characterized and therefore is a prime target for studying principles of neural circuit dynamics.

Since the early 1900's, the principal evidence for the understanding of the praxis network in the brain has been developed from lesion studies of adults with acquired apraxia. Acquired ideomotor apraxia manifests as the inability to perform or pantomime communicative gestures (e.g., waving good-bye) and tool-use gestures (e.g., brushing teeth), despite normal basic motor skills (including strength and coordination). Through systematic study of performance deficits in patients with a variety of anatomical lesions, a hierarchical model has been proposed which establishes putative information transformations at various anatomical regions within the praxis network (Heilman and Valenstein, 2003). Both visual and auditory regions may serve as input into praxis-specific regions of the network, which are typically lateralized to the left hemisphere and include left inferior parietal cortex, which is believed to contain a "praxicon" (analogous to a lexicon), in which sensori-motor representations of praxis gestures are stored. Lesions of this area result in deficits both in the production of praxis gestures and in the recognition of praxis gestures produced by others. During the production of gestures, sensori-motor representations or "programs" are believed to be transmitted from left inferior parietal to left premotor regions (Heilman and Valenstein, 2003), where they are transcoded into signals compatible with primary motor cortex, where the gesture is executed. Frontal lesions tend to result in deficits in production but not in recognition of gestures. The overall dynamics of information propagation in the

brain during gesture production, as inferred from lesion studies, is thus understood to occur from parietal to frontal components of the praxis network.

While lesion studies have allowed investigators to infer the relationship between various regions, there has been relatively little direct physiological observation of the interactions between different cortical regions, using functional and effective connectivity techniques. Wheaton, Hallett and colleagues have demonstrated praxis-task-related activation of parietal and premotor regions as well as event-related functional connectivity between anatomical areas (specifically parietal and premotor) that constitute the network (Wheaton et al., 2005a, Wheaton et al., 2005b, Wheaton et al., 2008, Wheaton et al., 2009).

To study the interactions among the various regions of the human praxis network, we used measures of effective connectivity to examine causal interactions between nodes in the network at behaviorally relevant time scales. “Effective connectivity” measures show directed (“causal”) interactions between brain regions, derived from physiological time-series data, such as EEG (Friston, 1994, Behrens and Sporns, 2012).

We recorded scalp EEG in neuro-typical adults during the performance of a praxis task and tested two basic predictions from the classical hierarchical model of the human praxis network. First, this model predicts that the magnitude of activation and information propagation is greater in the left hemisphere than in the right. With few exceptions (Wheaton and Hallett, 2007), left-hemisphere lesions are responsible for acquired apraxia, and although physiological studies using fMRI and EEG have demonstrated bilateral activation, many of these studies demonstrate greater activation in the left (dominant) hemisphere (Moll et al., 2000, Wheaton et al., 2005a, Wheaton et al., 2005b, Bohlhalter et al., 2009). Second, as discussed above, the model predicts that the directionality of information propagation is primarily posterior-to-anterior, i.e., from parietal to premotor regions.

Based on the classical model, we therefore hypothesized that neural activation and propagation accompanying praxis task would be greater in magnitude in the left hemisphere than the right, and that propagation would be directed from posterior to anterior regions.

2. Materials and Methods

2.1 Participants

Seventeen right-handed (based on self-report) adult subjects (10 male, 7 female) at least 18 years of age (mean age = 26.18, SD = 4.17) participated in the study. Volunteers were screened to exclude individuals with neurological or psychiatric disorders. Each session lasted 1–1.5 hours. Informed consent was obtained, and participants were compensated with a $25 gift card for their participation. The protocol was approved by Johns Hopkins Medicine Institutional Review Board.

2.2 Task

The task was largely based on the paradigm from Wheaton *et al* (2005) and consisted of the pantomime of using 10 common tools (scissors, spoon [to stir coffee], ice cream scoop,

doorknob, pencil, screwdriver, hammer, paintbrush, key, chalkboard eraser). These tools were selected because the pantomime of their use would allow the participant to keep his or her elbow on the chair's armrest, thus minimizing movement artifact in the EEG recording. Prior to the recording, the participants were asked to demonstrate the correct use of each of the tools. During the EEG recording, the stimuli were presented using eevoke software (ANT, the Netherlands). During the pre-stimulus portion of each trial, subjects first fixated on a cross at the center of the computer monitor; this stimulus lasted four seconds (Fig. 1). The fixation cross was replaced by the photograph of one of the ten tools, each with a size on the monitor that intersected 9 degrees of visual angle; participants were instructed not to make any movements during this time. We refer to this first stimulus as the "*Prepare*" stimulus. After this *Prepare* stimulus remained on the screen for three seconds, a green box appeared around the photograph of the tool ("*Go*" stimulus). During the presentation of the *Go* stimulus (which lasted 3.5 sec), subjects pantomimed the use of the tool with their right hand until the word "Rest" appeared. "Rest" lasted two seconds and was replaced by the fixation cross for the next trial. 100–160 trials were recorded in each subject, with the experimenter continuously observing performance. Accuracy in the performance of praxis movements approached 100% for all subjects, and no trials were removed for behavioral performance errors. The period following the *Prepare* stimulus was presumed to elicit covert motor imagination or rehearsal, while the period following *Go* required the performance of a tool-use gesture.

2.3 Recordings

The EEG data were recorded from 128 sites covering the whole scalp with approximately uniform density, using a high density elastic electrode cap (Waveguard cap with 128-channel Duke [equidistant electrode placement] layout, made by Advanced Neuro Technology [ANT], the Netherlands; see Fig. 2). The recording was performed in DC mode, with a 512 Hz sampling rate and an anti-aliasing filter with a 138Hz cut off. Each channel was referenced to an average of all channels during recording. The electrode cap used active cable-shielding technology. Electrode impedance was kept below 5 kΩ in all channels.

2.4 Signal Pre-Processing

All EEG data were visually inspected, and channels with artifacts persistent throughout the recording were excluded. Very few channels were excluded from any subject (average = 1.3, maximum = 7). Signals were re-referenced to new average references (specific to the type of analysis, as described below), but the excluded channels were removed from all references used. Vertical electro-oculograms (VEOG) were recorded on-line from frontal channels whose locations were designed specifically to capture eye blinks. Eye blink correction was then performed using a principal component analysis (PCA) method that models the brain signal and artifact subspaces (Ille et al., 2002). Specifically, we asked subjects to blink naturally during the EEG recording, and prior to the start of praxis experiment. We then visually identified and marked several definite eyeblinks in each subject. The PCA algorithm identified components specific to these eyeblinks and then searched the remainder of the record for matching components. It then removed the first one or several principal components specific to the eyeblinks, leaving the remainder of the activity intact. The horizontal eye movement artifacts (HEOG), which were picked up by the cap electrodes

(LE1 and RE1) located 1–2 cm lateral to external epicanthi, were removed if the amplitude exceeded a threshold defined individually for each subject (based on analysis of definite horizontal eye movements). EEG data from each trial was time-locked to the onset of the *Prepare* stimulus. Epochs were created with a pre-stimulus (baseline) length of 1.2 sec and post-*Prepare*-stimulus-onset (trial) length of 6.8 sec, for a total length of 8 sec. Trials with excessive muscle or movement artifact were removed; 5.06 ± 5.68 (mean ± SD) trials were removed per subject. Current source density (CSD) estimates for the surface potentials were then computed using the spherical spline algorithm (Kayser and Tenke, 2006). As described below, preliminary spectral analysis using Matching Pursuit showed strong event-related increases of signal power in the 2–10 Hz frequency range in all subjects. Although both alpha (Pfurtscheller and Neuper, 1994) and beta (Engel and Fries, 2010) event-related desynchronization (ERD) are known to be associated with motor planning and execution, we focused this analysis on the 2–10 Hz range because in this range we consistently observed the strongest event-related synchronization (ERS) forming separate topographical clusters in the parietal regions during praxis preparation and in the frontal regions during praxis execution, with a natural boundary in activity between the parietal and frontal regions (Fig. 3), as described in section 3.1. Therefore, for further analyses, signals were band-pass filtered (2–10 Hz) with an FIR filter. To avoid phase shift, the EEG signals were filtered twice (back and forth). They were then down-sampled (decimated) by 2 to 256 Hz (to avoid oversampling for the analyzed frequency band, but to preserve time resolution high enough to investigate quick activity propagations between channels).

2.5 Matching Pursuit

In order to confirm task-related cortical regional activation and identify topographical regions of interest as well as the relevant frequency band for effective connectivity analysis, we looked for event-related changes in EEG spectral power by performing a broad-band, high-time-resolution spectral analysis. For this, we used the matching pursuit (MP) algorithm, implemented in custom analysis interface (ANIN) software (Mallat and Zhang, 1993, Jouny et al., 2003, Franaszczuk and Jouny, 2004, Jouny et al., 2007, Boatman-Reich et al., 2010). Event-related synchronization (ERS) is a term used to refer to task-related increases in the power of the signal with a given frequency range. It is presumed to result from increased synchronization of activity in neuronal ensembles recorded by a given EEG channel. ERS in theta/alpha frequencies, including those analyzed here, is commonly observed during task-related processing (Klimesch, 1999, Kahana et al., 2001, Ekstrom et al., 2005, Onton et al., 2005, Sauseng et al., 2005, Sauseng et al., 2007, Capotosto et al., 2009, Kostandov et al., 2010) and may reflect integration of processing across different brain regions (Pfurtscheller, 2006).

MP is an iterative procedure that decomposes a signal $x(t)$ into a linear combination of members of a specified set of functions. In this study we used a dictionary of cosine-modulated Gaussians (Gabor functions), cosines, and Dirac delta functions. Gabor functions provide the best compromise between time and frequency resolution, to the extent allowed by the uncertainty principle. Cosines were added to the dictionary for better representation of rhythmic components with constant amplitude, and a Dirac delta was added to represent very short transients. This algorithm performs adaptive approximation of energy density for

both stationary and non-stationary signals, which makes it preferable over alternative methods, including short-time Fourier transform and wavelet decomposition. The MP method is particularly well suited for analysis of rapidly changing signals and is appropriately applied to signals with linear or nonlinear characteristics.

The energy distribution for each time-sample after stimulus onset, drawn from all good trials (task repetitions), was compared to the distribution of all time-points of the pre-stimulus baseline period, also drawn from all good trials, using *t*-test with significance level 0.05 and false discovery rate (FDR) correction for multiple comparisons. To develop the grand average, the values of significant increases in signal energy (ERS) were averaged over all selected channels in each ROI (see Section 2.6, below), normalized to the value of 1, and averaged across subjects.

2.6 ROI and Channel Selection

Visual inspection of both single-subject and grand average MP plots showed that a "discontinuity" existed between channels in the central scalp regions (whose activity is presumed to come from frontal regions) and channels in the posterior scalp regions (whose activity is presumed to come from parietal regions) (Fig. 3). Specifically, the parietal channels revealed high ERS during the 0–1 sec interval and smaller ERS during the 3–4 sec interval, while the frontal channels revealed lower ERS during the 0–1 sec interval and the higher ERS during 3–4 sec interval. We selected the border between frontal and parietal ROIs based on grand-averaged data. This border comported well with the discontinuity in ERS activity between central and posterior regions in individual single-subject analyses.

For each channel, an integral was calculated from ERS over the frequency range of 2–10 Hz, separately over the time ranges of 0–1s and 3–4s. For each subject individually, we then selected six channels in each ROI that had the greatest integrated ERS. The midline electrodes were also removed from the analysis, as it would be unclear as to whether they should go into the left or right ROI. Channels in the parietal ROIs were ranked based on integrated ERS during the 0–1 sec *Prepare* phase, as ERS in the parietal regions was greater in magnitude during the *Prepare* than *Go* phase, as described below. Channels in the frontal ROIs were ranked based on ERS in the 3–4 sec *Go* phase, as ERS was greater in magnitude the frontal regions during the *Go* than *Prepare* phase. The top six channels were selected in each of the four ROIs. By selecting the same number of channels in each ROI, we eliminate the potential bias in coherence and propagation magnitudes associated with having an uneven number of channels in different ROIs. The rationale for selecting six channels is based on the limitations of the ERC technique and is described below.

To assess laterality and left *vs*. right differences in ERS, we computed values in each subject for each ROI in both the 0–1 sec and 3–4 sec time window by integrating ERS for 2–10 Hz. Using a paired Student's *t*-test, we then compared across subjects left *vs*. right, and frontal *vs*. parietal ROIs, separately, for both 0–1 sec and 3–4 sec time windows. Based on the classical brain model of praxis, we predicted a left > right laterality.

2.7 Coherence

Prior to assessing *effective* connectivity, we first examined event-related changes in functional connectivity (ERFC), using coherence (Jenkins and Watts, 1968, Bendat and Piersol, 1971), a widely used technique in EEG. Functional connectivity refers to the assessment, using physiological measures, of time-dependent correlations between signals: neural systems that "fire" together are presumed to be wired (and working) together (Behrens and Sporns, 2012). In order to measure ERFC, we computed the magnitude squared coherence (with "mscohere" function implemented in MATLAB) using Welch's average periodogram method between each channel and every other channel. Coherence is a measure of the degree of association or coupling of power spectra between two different time series and is defined as the normalized cross-power spectrum. The temporal evolution of these estimates was obtained by calculating coherence in Hamming windows of length 256 msec with 50% overlap.

In order to compute the average coherence between any two ROIs, the coherence was computed for seven seconds (−1 sec to 6 sec relative to the onset of the *Prepare* stimulus) for each channel in the first ROI × each channel in the second ROI ($6^2 = 36$ pairs). For each of these 36 coherence time series, we next normalized the coherences to the pre-*Prepare* stimulus baseline, and compared left *vs*. right, and parietal *vs*. frontal pairs of ROIs using a Student's *t*-test. The average coherence between ROIs therefore represented the average of the 36 channel-pair coherence time series. The average coherence waveforms were computed by averaging across subjects, after each ROI pair coherence time series was normalized to 1. Statistics (Student's *t*-test) were then calculated across subjects. In particular, we predicted that ERFC would be of a greater magnitude on the left (as compared with the right) during both *Prepare* and *Go* phases.

2.8 Short-time direct Directed Transfer Function and Event Related Causality

Effective connectivity among cerebral networks can be measured by a recently developed technique, Short-time direct Directed Transfer Function (SdDTF) (Korzeniewska et al., 2008). SdDTF is based on estimation of a multivariate autoregresssive model (MVAR), which uses past observations in recorded signals to describe current values in these signals. SdDTF is based on the concept of Granger causality, in which one can consider an observed time series $x(t)$ to have a causal effect on another time series $y(t)$ if knowledge of $x(t)$'s past significantly improves prediction of $y(t)$ (Granger, 1969). SdDTF gives an estimate of the direction and intensity of interactions between recording sites as a function of frequency and time, and it measures only direct causal interactions, i.e., excluding the influence of indirect interactions (as mediated by other recording sites/brain areas) (Korzeniewska et al., 2003, Korzeniewska et al., 2008). Event-Related Causality (ERC) is… a Granger Causality-concept-based effective connectivity assessment method that has been validated in electrocorticography (ECoG) research (Kaminski and Blinowska, 1991, Korzeniewska et al., 2008, Blinowska, 2011), (Kaminski and Blinowska, 1991, Ginter et al., 2001, Blinowska, 2011). It builds on the direct Directed Transfer Function (dDTF) (Korzeniewska et al., 2003) and, specifically, short-time direct DTF (SdDTF) (Korzeniewska et al., 2008). This family of methods has a specific advantage in scalp EEG over other effective connectivity measures

in that it mitigates the effects of volume conduction by minimizing the effect of zero-phase-delay conduction.

To evaluate the spatial-temporal course of brief changes in patterns of effective connectivity, we used multivariate autoregressive (MVAR) algorithm introduced by Ding *et al* (Ding et al., 2000). The temporal evolution of these estimates was obtained by calculating SdDTF in short windows of 0.6 sec, shifted in time by 0.02 sec, for multiple realizations of the same stochastic process (many trials/repetitions of the task). Multiple trials or task repetitions from the same subject may be treated as repeated realizations of the same stochastic process which is stationary over short periods.

For SdDTF analyses, only 24 signals (6 in each ROI) with the highest ERS magnitudes were selected for each subject as described above, due to the requirements of the ERC method, which has a natural trade-off between number of channels, number of trials, and time resolution (as described in Korzeniewska et al. 2008). For the ERC analysis, we used the same channels that were selected for the coherence analysis as described above. The pre-processed signals were band-pass filtered (2–10 Hz), down-sampled to 256 Hz, and normalized over time by subtracting their mean and dividing by their standard deviation in each channel, and in each window (Korzeniewska et al., 2008). For each set of the multiple recordings, a common MVAR-model order was determined using Akaike information criterion (AIC) with a correction for finite sample size. The coefficients were calculated by solving Yule-Walker equations, using the Levinson-Wiggins-Robinson algorithm, and estimates of cross-correlation matrices were based on all available trials.

To test the statistical significance of task-related (event-related) changes in SdDTF, we applied an event-related causality (ERC) method (Korzeniewska et al., 2008), which statistically tests differences in smoothed SdDTF between baseline and post-stimulus periods. Thus, ERC is designed to estimate the intensity, directionality, spectral characteristics, and time course of statistically significant event-related changes in causal interactions or activity propagations between recording sites. In this study the threshold for statistical significance was set as $p = 0.05$ (95% confidence interval) after applying Bonferroni correction for multiple comparisons.

Next, ERC values were integrated over the analyzed frequency band (2–10 Hz) and time intervals of 1 sec duration (0–1 sec, 1–2 sec, …, 5–6 sec) following the onset of the *Prepare* stimulus for all propagations between each of the recording sites within a pair of ROIs, and normalized to the number of propagations. ERC results were individually rescaled for each subject to the value of 1 and then averaged over subjects to develop the grand average.

To examine statistical relationships among propagations between ROIs, we summed, within each subject, the propagations from one ROI to each other. Statistics (paired Student's *t*-test) were then calculated across subjects. Based on the classical model, we tested the hypothesis that activity propagations occur predominantly in the left hemisphere, directed from parietal to frontal cortex (i.e., parietal to frontal ROIs).

3. Results

3.1 Event Related Synchronization (ERS)

Event-related time-frequency analyses, performed using matching pursuit (MP), consistently demonstrated strong, statistically significant event-related synchronization (ERS) in the frequency range of 2–10 Hz in electrodes in separate topographical clusters in the frontal and parietal regions (Fig. 3). Using an initial broad band MP analysis (2–25 Hz), we also observed mu-frequency and beta-frequency ERD related to *Prepare* and *Go* (Pfurtscheller and Neuper, 1994) with timing linked to the task. Unlike the 2–10 Hz ERS, for which there was a natural boundary in activity between central and posterior regions (Fig. 3, see also section 2.5 in Methods), the beta and mu ERD activity occurred in a single cluster in central scalp regions, in both single-subject and grand average analyses. Given that there was no clear way to divide the beta and mu into distinct topographical regions as a preliminary step to measuring connectivity between those regions, our functional and effective connectivity measurements were focused on the 2–10 Hz band.

In the MP analysis, 2–10 Hz ERS was seen for approximately one second following the *Prepare* stimulus (0–1 sec into the task) and again for one second following the *Go* stimulus (3–4 sec into the task). Figure 4 shows ERS averaged across all subjects and across all electrodes of each region of interest. There were significant anterior/posterior effects. Following *Prepare*, ERS magnitudes were significantly greater in left ($p < 0.001$) and right ($p < 0.001$) parietal ROIs than in the corresponding frontal ROIs. Moreover, in both left and right parietal ROIs, ERS magnitudes were significantly greater following *Prepare* than following *Go* ($p < 0.001$ in both cases). Further, ERS magnitude in the left frontal ROI following *Go* was significantly greater ($p < 0.001$) than following *Prepare*. ERS magnitude following *Go* was significantly greater ($p < 0.001$) in the left frontal ROI than in the right frontal ROI. Both of these phenomena presumably reflect left motor cortex activation associated with gesturing in the right hand.

3.2 Event-Related Functional Connectivity (ERFC)

Task-related temporal changes in functional connectivity (as indexed by 2–10 Hz coherence) were apparent for each pair of ROIs (Fig. 5, Table 1). As with ERS, the peaks observed in ERFC for 0–1 sec and 3–4 sec were significantly higher in comparison to the pre-stimulus baseline and closely followed the timing of the *Prepare* and *Go* stimuli. In the one second period following onset of the *Prepare* stimulus, the coherence increase between left and right parietal ROIs (LP-RP) was significantly higher ($p = 0.011$) than that seen in the second following *Go*. This again may reflect integration of processing between visual areas in each hemisphere and/or the left parietal praxis area and its right-sided homologue, as described in previous studies of object recognition (Mima et al., 2001). There was no statistical laterality difference in coherence (LP↔LC *vs*. RP↔RC) after either *Prepare* or *Go*.

3.3 Effective Connectivity

Both temporal and spatial effects were observed as task-related changes in effective connectivity, as revealed by ERC. Grand averages of ERC results are shown in Fig. 6. The arrows shown are a graphical representation of statistically significant increases in

directional propagations as compared with baseline, thus propagation evoked by the performed task. As a first observation, and consistent with the task timing, the total integrated magnitude of propagations was significantly greater in the 0–1 sec time range (following onset of the *Prepare* stimulus) and the 3–4 sec range (following onset of the *Go* stimulus) than in all other 1-second bins.

Second, we compared ERC to ERFC. Consistent with ERFC results, ERC analysis showed greater propagation between parietal ROIs (LP↔RP) following the onset of *Prepare* as compared with the second following onset of *Go* ($p = 0.011$). Further, in the 0–1 sec range, the propagations between parietal regions was greater than the propagations between frontal ROIs (LF↔RF, $p = 0.0036$). These observations again likely reflected activity in the visual system or between the left parietal praxis area and its homologue on the right during the motor preparation phase. Bidirectional propagations in the frontal regions (LF↔RF) were greater following onset of *Go* than following the onset of *Prepare* ($p = 0.011$), perhaps reflecting the activity of the motor system during gesture execution.

Third, we examined laterality in the ERC results. Based on lesion studies that demonstrate that *left* hemisphere brain regions are necessary for praxis function, we predicted that propagations within the left hemisphere would be greater than propagations within the right. Although we observed a trend for greater parietal-to-frontal propagation on the left than on the right, there was not a statistically significant difference. However, we did observe statistically significant directionality of propagation that occurred during the *Prepare* phase in the left hemisphere, but not in the right. Specifically, propagation from left parietal to left (and right) frontal regions was significantly greater than propagations in the opposite directions ($p < 0.05$). No such directional asymmetry occurred on the right. Moreover, the left parietal region was a net source of propagations during this time period (i.e., all out-flows from that ROI were greater than all in-flows into the ROI; $p = 0.013$). Further, the left frontal ROI was a net sink for propagations during this time period (i.e., all in-flows were greater than all out-flows; $p = 0.0137$). Neither of the right-sided ROIs was a net source or sink during *Prepare*, and no ROI was a net source or sink during *Go*. In addition, at 3–4 sec, there were no significant left *vs*. right differences in any comparisons.

4. Discussion

We observed similar dynamics for functional and effective connectivity during our experimental praxis task. That is, both indices increased during the second after the *Prepare* and *Go* cues relative to other time periods. This finding is non-trivial because ERFC methods include simultaneous synchronization in their estimates, whereas the ERC method specifically excludes it.

The expected lateralization of overall magnitude of praxis network activity was not statistically significant, though there was a trend toward left lateralization of effective connectivity. Nevertheless, when the *directionalities* of changes in effective connectivity were taken into account, we observed an anterior-posterior directional predominance in parietal-frontal propagation in the left hemisphere, but not in the right. These findings

suggest that the directionality of effective connectivity may help uncover significant properties of the system that are lost by examining only its functional connectivity.

Effective connectivity measures provided a number of additional insights about the dynamics of the praxis network. First, rather than demonstrating simple left parietal-to-frontal propagation, as would be the most parsimonious prediction from the hierarchical model, activity within the praxis network was somewhat more complex. Specifically, mental imagery/preparation (i.e., activity following the onset of *Prepare*) was also associated with propagation from left parietal to right frontal regions.

When viewed in the context of previous studies of the human praxis network, our results may be interpreted as evidence for directionally specific influences among broadly defined modules of this network during different phases of the praxis task. During the *Prepare* phase, propagations from the left parietal ROI to the left frontal ROI may reflect the influence of a visual-kinesthetic representation of the gesture, selected from the praxicon in left parietal cortex, on preparation of motor responses to be implemented during the *Go* phase. During the *Go* phase, frontal-to-parietal propagations might represent a neurophysiological signature of corollary discharges from motor cortex to parietal cortex, providing it with a forward model of the proprioceptive feedback that is predicted as a consequence of executed motor commands. Similar feedback structures have been proposed in studies of motor adaptation using other types of tasks (Wolpert and Miall, 1996, Shadmehr and Krakauer, 2008). Simultaneous parietal-to-frontal propagation during execution may reflect updating of the motor program based on mismatch between the efference copy and perceptual feedback. This ongoing interaction between frontal and parietal regions during motor preparation and execution could help explain the presence of bilateral posterior responses during both go and no-go conditions in prior experiments (Wheaton et al., 2009) that would not be predicted by the classical model of praxis function. Indeed, the current evidence suggests that, unlike the serial propagation of information from parietal to frontal areas predicted by the simplest formulation of the classical model of praxis network function, there are more complex interactions that accommodate important sensory-motor feedback mechanisms.

These data also present a unique insight into the nature of the interactions between neural systems in the left and right hemispheres during praxis planning and execution. The classical model, based primarily on neuropsychological lesion data, stresses the primacy of left hemispheric regions (Heilman and Valenstein, 2003, Wheaton and Hallett, 2007) though physiological data demonstrate a bilateral network (albeit one in which magnitudes of activation are higher on the left) (Moll et al., 2000, Johnson-Frey et al., 2005, Bohlhalter et al., 2009).

Based on this, one might propose a model in which the left parietal and left premotor regions operate as one unit, while their right-sided homologues operate as a separate unit. An alternative model is that the frontal-parietal network nodes interact with one another. Our results provide support for this latter account. Specifically, we observed strong “diagonal” propagation, from left parietal to right frontal regions, and propagations from left to right parietal ROI as well as propagations from left to right frontal ROI. Rare cases of callosal

apraxia from lesions of the corpus callosum (Goldenberg et al., 2001) have been hypothesized to arise by disconnection of right parietal and left premotor regions. Our observations may represent the first physiological evidence for effective connectivity between these components of the praxis network.

The overall role of the right hemisphere in praxis function, however, is not well understood. Whereas most lesion studies confirm the necessity of the left hemisphere (Heilman and Valenstein, 2003, Wheaton and Hallett, 2007), physiological studies consistently report activation of the right hemisphere (Moll et al., 2000, Wheaton et al., 2005a, Wheaton et al., 2005b, Bohlhalter et al., 2009). Further, there have been some descriptions of apraxia due solely to right hemisphere lesions (Wheaton and Hallett, 2007). The exact nature of the processing occurring in the right hemisphere is however unknown. While it is possible that it is limited to visuomotor integration, the high level of interaction between the left and right hemispheres, including both posterior *and* anterior regions, suggests that the right hemisphere may play a greater role.

While previous studies using ERC to examine human network dynamics have used intracranially recorded high gamma activity (80–120 Hz) (Korzeniewska et al., 2011), the current analyses demonstrate propagation of neural activity at lower frequency activities (2–10 Hz). The signal characteristics of the scalp EEG signal prevented us from examining high gamma activity or correlating this activity with the propagations we observed at lower frequencies. However, recent studies have demonstrated modulation of high gamma activity by the phase of theta/alpha activity (4–12 Hz) (Bragin et al., 1995, Chrobak and Buzsaki, 1998, Sederberg et al., 2003, Lakatos et al., 2005, Canolty et al., 2006, Sauseng et al., 2008, Griesmayr et al., 2010, Sauseng et al., 2010, Voytek et al., 2010), and it is intriguing to speculate that propagated low frequency oscillations could facilitate the coordination of neural population activity reflected at higher frequencies (Crone et al., 2011). Future work combining ECoG and scalp EEG data or using magnetoencephalography (MEG) data may better clarify the potential role of gamma/high-gamma activity as it relates to praxis network function as well as the functional relationship between theta/alpha and gamma.

Although we can draw provisional conclusions from the present study about the frontal-parietal and left-right dynamics of the praxis network, further work using a variety of experimental paradigms will be needed to understand more deeply the relative contribution of the various nodes of this network and to evaluate alternative explanations. For example, the assumption that the activity recorded following the first stimulus represents mental preparation/rehearsal, although supported anecdotally by self-report from participants, may be incorrect. Additionally, the role of sensory input can be further defined by experiments in which sensory cues are delivered via the visual system or the auditory system (or are internally initiated) and via control experiments. Another potential confound is that the gestures were performed only with the right hand, and this might have biased the laterality of the ERC results to favor the left side. However, if it were indeed the case that there is truly no laterality to the praxis system and that any observed laterality in the results was due solely to responses being made with the left hand, we would have expected to observe propagation from both left and right parietal regions to the left frontal region during preparation. Instead, we observed propagation from the left parietal region to both left and

right frontal regions, and this left > right bias in the parietal outflow suggests the greater contribution of the left hemisphere. Future work may examine gesture production with alternating hands to assess the meaning of the observed laterality even more rigorously.

In summary, we report the first study of the dynamics of effective connectivity in the praxis network of normal adult humans. The ERC technique demonstrated patterns of task-related causal interactions consistent with the known spatial topography of the praxis network. The added dimension of directionality permitted by this technique characterized network dynamics that were not captured by functional connectivity. In particular, this technique revealed directionally specific propagation from parietal to frontal regions during the preparation stage in the left hemisphere, but not in the right. Indeed, the left parietal region was the most prominent source of propagation across the praxis network. Our observations here may also provide direct human physiological evidence of corollary discharge in the frontal-parietal praxis network, consistent with current motor control theory (Wolpert and Miall, 1996).

Acknowledgements

This work was supported by the National Institutes of Neurological Disorders and Stroke at the National Institutes of Health (grant numbers K23 NS073626 to J.B.E., R01 NS048527 to S.H.M., and R01 NS40596 to N.E.C.; Intramural Program to M.H.) and Autism Speaks (to S.H.M.). Dr. Hallett is supported by the NINDS Intramural Program. The study sponsors had no role in collection, analysis or interpretation, or in the preparation of the manuscript.

References

Behrens TE, Sporns O. Human connectomics. Curr Opin Neurobiol. 2012; 22:144–153. [PubMed: 21908183]

Bendat, JS.; Piersol, AG. Random data: Analysis and measurement procedures. New York: Wiley - Interscience; 1971.

Blinowska KJ. Review of the methods of determination of directed connectivity from multichannel data. Med Biol Eng Comput. 2011; 49:521–529. [PubMed: 21298355]

Boatman-Reich D, Franaszczuk PJ, Korzeniewska A, Caffo B, Ritzl EK, Colwell S, et al. Quantifying auditory event-related responses in multichannel human intracranial recordings. Front Comput Neurosci. 2010; 4:4. [PubMed: 20428513]

Bohlhalter S, Hattori N, Wheaton L, Fridman E, Shamim EA, Garraux G, et al. Gesture subtype-dependent left lateralization of praxis planning: an event-related fMRI study. Cereb Cortex. 2009; 19:1256–1262. [PubMed: 18796430]

Bragin A, Jando G, Nadasdy Z, Hetke J, Wise K, Buzsaki G. Gamma (40–100 Hz) oscillation in the hippocampus of the behaving rat. J Neurosci. 1995; 15:47–60. [PubMed: 7823151]

Canolty RT, Edwards E, Dalal SS, Soltani M, Nagarajan SS, Kirsch HE, et al. High gamma power is phase-locked to theta oscillations in human neocortex. Science. 2006; 313:1626–1628. [PubMed: 16973878]

Capotosto P, Perrucci MG, Brunetti M, Del Gratta C, Doppelmayr M, Grabner RH, et al. Is there "neural efficiency" during the processing of visuo-spatial information in male humans? An EEG study. Behav Brain Res. 2009; 205:468–474. [PubMed: 19665491]

Chrobak JJ, Buzsaki G. Gamma oscillations in the entorhinal cortex of the freely behaving rat. J Neurosci. 1998; 18:388–398. [PubMed: 9412515]

Crone NE, Korzeniewska A, Franaszczuk PJ. Cortical gamma responses: searching high and low. Int J Psychophysiol. 2011; 79:9–15. [PubMed: 21081143]

Ding M, Bressler SL, Yang W, Liang H. Short-window spectral analysis of cortical event-related potentials by adaptive multivariate autoregressive modeling: data preprocessing, model validation, and variability assessment. Biol Cybern. 2000; 83:35–45. [PubMed: 10933236]

Ekstrom AD, Caplan JB, Ho E, Shattuck K, Fried I, Kahana MJ. Human hippocampal theta activity during virtual navigation. Hippocampus. 2005; 15:881–889. [PubMed: 16114040]

Engel AK, Fries P. Beta-band oscillations--signalling the status quo? Curr Opin Neurobiol. 2010; 20:156–165. [PubMed: 20359884]

Franaszczuk P, Jouny C. Software system for data management and distributed processing of multichannel biomedical signals. Software system for data management and distributed processing of multichannel biomedical signals. 2004; 26:983–985.

Friston KJ. Functional and effective connectivity in neuroimaging: A synthesis. Human Brain Mapping. 1994; 2:56–78.

Ginter J Jr, Blinowska KJ, Kaminski M, Durka PJ. Phase and amplitude analysis in time-frequency space--application to voluntary finger movement. J Neurosci Methods. 2001; 110:113–124. [PubMed: 11564531]

Goldenberg G, Laimgruber K, Hermsdorfer J. Imitation of gestures by disconnected hemispheres. Neuropsychologia. 2001; 39:1432–1443. [PubMed: 11585611]

Granger C. Investigating Causal Relations by Econometric Models and Cross-Spectral Methods. Econometrica. 1969; 37:424–438.

Griesmayr B, Gruber WR, Klimesch W, Sauseng P. Human frontal midline theta and its synchronization to gamma during a verbal delayed match to sample task. Neurobiol Learn Mem. 2010; 93:208–215. [PubMed: 19808098]

Heilman, KM.; Valenstein, E. Clinical neuropsychology. 4th ed.. Oxford; New York: Oxford University Press; 2003.

Ille N, Berg P, Scherg M. Artifact correction of the ongoing EEG using spatial filters based on artifact and brain signal topographies. J Clin Neurophysiol. 2002; 19:113–124. [PubMed: 11997722]

Jenkins, GM.; Watts, DG. Spectral analysis and its applications. San Francisco: Holden-Day; 1968.

Johnson-Frey SH, Newman-Norlund R, Grafton ST. A distributed left hemisphere network active during planning of everyday tool use skills. Cereb Cortex. 2005; 15:681–695. [PubMed: 15342430]

Jouny CC, Adamolekun B, Franaszczuk PJ, Bergey GK. Intrinsic ictal dynamics at the seizure focus: effects of secondary generalization revealed by complexity measures. Epilepsia. 2007; 48:297–304. [PubMed: 17295623]

Jouny CC, Franaszczuk PJ, Bergey GK. Characterization of epileptic seizure dynamics using Gabor atom density. Clin Neurophysiol. 2003; 114:426–437. [PubMed: 12705423]

Kahana MJ, Seelig D, Madsen JR. Theta returns. Curr Opin Neurobiol. 2001; 11:739–744. [PubMed: 11741027]

Kaminski MJ, Blinowska KJ. A new method of the description of the information flow in the brain structures. Biol Cybern. 1991; 65:203–210. [PubMed: 1912013]

Kayser J, Tenke CE. Principal components analysis of Laplacian waveforms as a generic method for identifying ERP generator patterns: I. Evaluation with auditory oddball tasks. Clin Neurophysiol. 2006; 117:348–368. [PubMed: 16356767]

Klimesch W. EEG alpha and theta oscillations reflect cognitive and memory performance: a review and analysis. Brain Res Brain Res Rev. 1999; 29:169–195. [PubMed: 10209231]

Korzeniewska A, Crainiceanu CM, Kus R, Franaszczuk PJ, Crone NE. Dynamics of event-related causality in brain electrical activity. Hum Brain Mapp. 2008; 29:1170–1192. [PubMed: 17712784]

Korzeniewska A, Franaszczuk PJ, Crainiceanu CM, Kus R, Crone NE. Dynamics of large-scale cortical interactions at high gamma frequencies during word production: event related causality (ERC) analysis of human electrocorticography (ECoG). Neuroimage. 2011; 56:2218–2237. [PubMed: 21419227]

Korzeniewska A, Manczak M, Kaminski M, Blinowska KJ, Kasicki S. Determination of information flow direction among brain structures by a modified directed transfer function (dDTF) method. J Neurosci Methods. 2003; 125:195–207. [PubMed: 12763246]

Kostandov EA, Cheremushkin EA, Kozlov MK. Evoked synchronization/desynchronization of cortical electrical activity in response to facial stimuli during formation of a set to an emotionally negative expression. Neurosci Behav Physiol. 2010; 40:421–428. [PubMed: 20339937]

Lakatos P, Shah AS, Knuth KH, Ulbert I, Karmos G, Schroeder CE. An oscillatory hierarchy controlling neuronal excitability and stimulus processing in the auditory cortex. J Neurophysiol. 2005; 94:1904–1911. [PubMed: 15901760]

Mallat SG, Zhang Z. Matching Pursuits with time-frequency dictionaries. IEEE Transactions on Signal Processing. 1993; 41:3397–3415.

Mima T, Oluwatimilehin T, Hiraoka T, Hallett M. Transient interhemispheric neuronal synchrony correlates with object recognition. J Neurosci. 2001; 21:3942–3948. [PubMed: 11356882]

Moll J, de Oliveira-Souza R, Passman LJ, Cunha FC, Souza-Lima F, Andreiuolo PA. Functional MRI correlates of real and imagined tool-use pantomimes. Neurology. 2000; 54:1331–1336. [PubMed: 10746606]

Mostofsky SH, Ewen JB. Altered connectivity and action model formation in autism is autism. Neuroscientist. 2011; 17:437–448. [PubMed: 21467306]

Onton J, Delorme A, Makeig S. Frontal midline EEG dynamics during working memory. Neuroimage. 2005; 27:341–356. [PubMed: 15927487]

Pfurtscheller G. The cortical activation model (CAM). Prog Brain Res. 2006; 159:19–27. [PubMed: 17071221]

Pfurtscheller G, Neuper C. Event-related synchronization of mu rhythm in the EEG over the cortical hand area in man. Neurosci Lett. 1994; 174:93–96. [PubMed: 7970165]

Sauseng P, Griesmayr B, Freunberger R, Klimesch W. Control mechanisms in working memory: a possible function of EEG theta oscillations. Neurosci Biobehav Rev. 2010; 34:1015–1022. [PubMed: 20006645]

Sauseng P, Hoppe J, Klimesch W, Gerloff C, Hummel FC. Dissociation of sustained attention from central executive functions: local activity and interregional connectivity in the theta range. Eur J Neurosci. 2007; 25:587–593. [PubMed: 17284201]

Sauseng P, Klimesch W, Gruber WR, Birbaumer N. Cross-frequency phase synchronization: a brain mechanism of memory matching and attention. Neuroimage. 2008; 40:308–317. [PubMed: 18178105]

Sauseng P, Klimesch W, Schabus M, Doppelmayr M. Fronto-parietal EEG coherence in theta and upper alpha reflect central executive functions of working memory. Int J Psychophysiol. 2005; 57:97–103. [PubMed: 15967528]

Sederberg PB, Kahana MJ, Howard MW, Donner EJ, Madsen JR. Theta and gamma oscillations during encoding predict subsequent recall. J Neurosci. 2003; 23:10809–10814. [PubMed: 14645473]

Shadmehr R, Krakauer JW. A computational neuroanatomy for motor control. Exp Brain Res. 2008; 185:359–381. [PubMed: 18251019]

Voytek B, Canolty RT, Shestyuk A, Crone NE, Parvizi J, Knight RT. Shifts in gamma phase-amplitude coupling frequency from theta to alpha over posterior cortex during visual tasks. Front Hum Neurosci. 2010; 4:191. [PubMed: 21060716]

Wheaton L, Fridman E, Bohlhalter S, Vorbach S, Hallett M. Left parietal activation related to planning, executing and suppressing praxis hand movements. Clin Neurophysiol. 2009; 120:980–986. [PubMed: 19345141]

Wheaton LA, Bohlhalter S, Nolte G, Shibasaki H, Hattori N, Fridman E, et al. Cortico-cortical networks in patients with ideomotor apraxia as revealed by EEG coherence analysis. Neurosci Lett. 2008; 433:87–92. [PubMed: 18249498]

Wheaton LA, Hallett M. Ideomotor apraxia: a review. J Neurol Sci. 2007; 260:1–10. [PubMed: 17507030]

Wheaton LA, Nolte G, Bohlhalter S, Fridman E, Hallett M. Synchronization of parietal and premotor areas during preparation and execution of praxis hand movements. Clin Neurophysiol. 2005a; 116:1382–1390. [PubMed: 15978500]

Wheaton LA, Shibasaki H, Hallett M. Temporal activation pattern of parietal and premotor areas related to praxis movements. Clin Neurophysiol. 2005b; 116:1201–1212. [PubMed: 15826863]

Wolpert DM, Miall RC. Forward Models for Physiological Motor Control. Neural Netw. 1996; 9:1265–1279. [PubMed: 12662535]

Highlights

- The dynamics of causal interactions in the praxis network of normal adult humans is reported for the first time.
- Directionally specific propagation from parietal to frontal regions is seen only in the left hemisphere.
- Our observations may provide physiological evidence of corollary discharge in the human frontal-parietal praxis network.

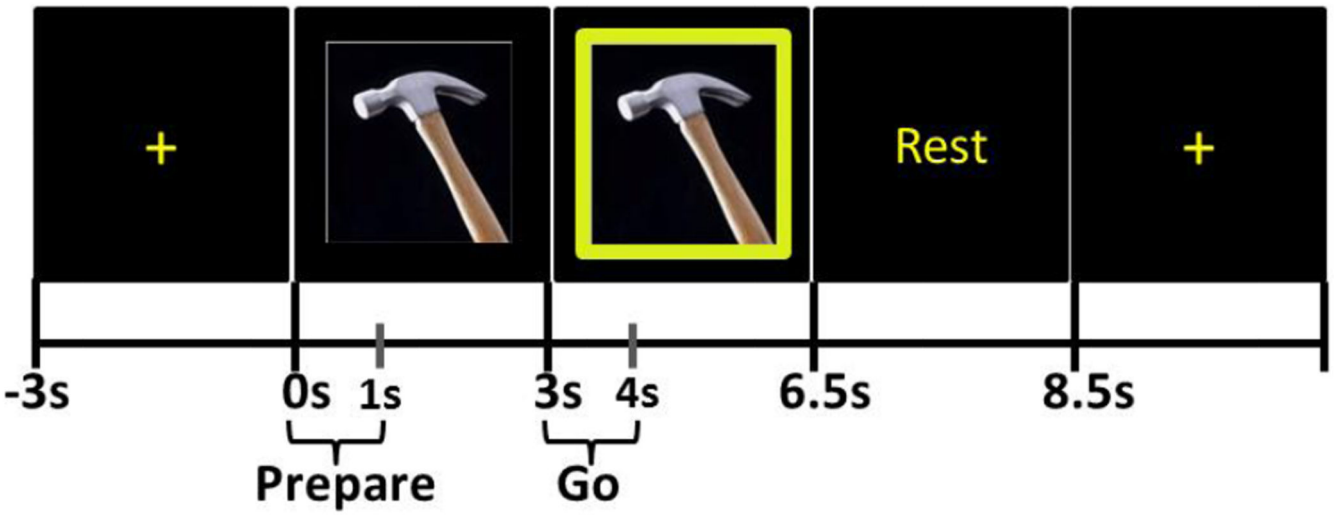

Figure 1. Tool-use task

The photograph immediately after the fixation cross is the *Prepare* stimulus, during the presentation of which subjects were instructed not to move. When the green frame appears around the photograph (*Go* stimulus), subjects pantomimed the use of the tool. Each trial was epoched from −1.2s (relative to the onset of *Prepare*; during the fixation cross) to +6.8s (after the onset of the *Rest* stimulus). The periods from 0–1s (relative to the onset of *Prepare*) and from 3–4s were used for subsequent analyses, based on results of Matching Pursuit analyses (described in Section 3.1).

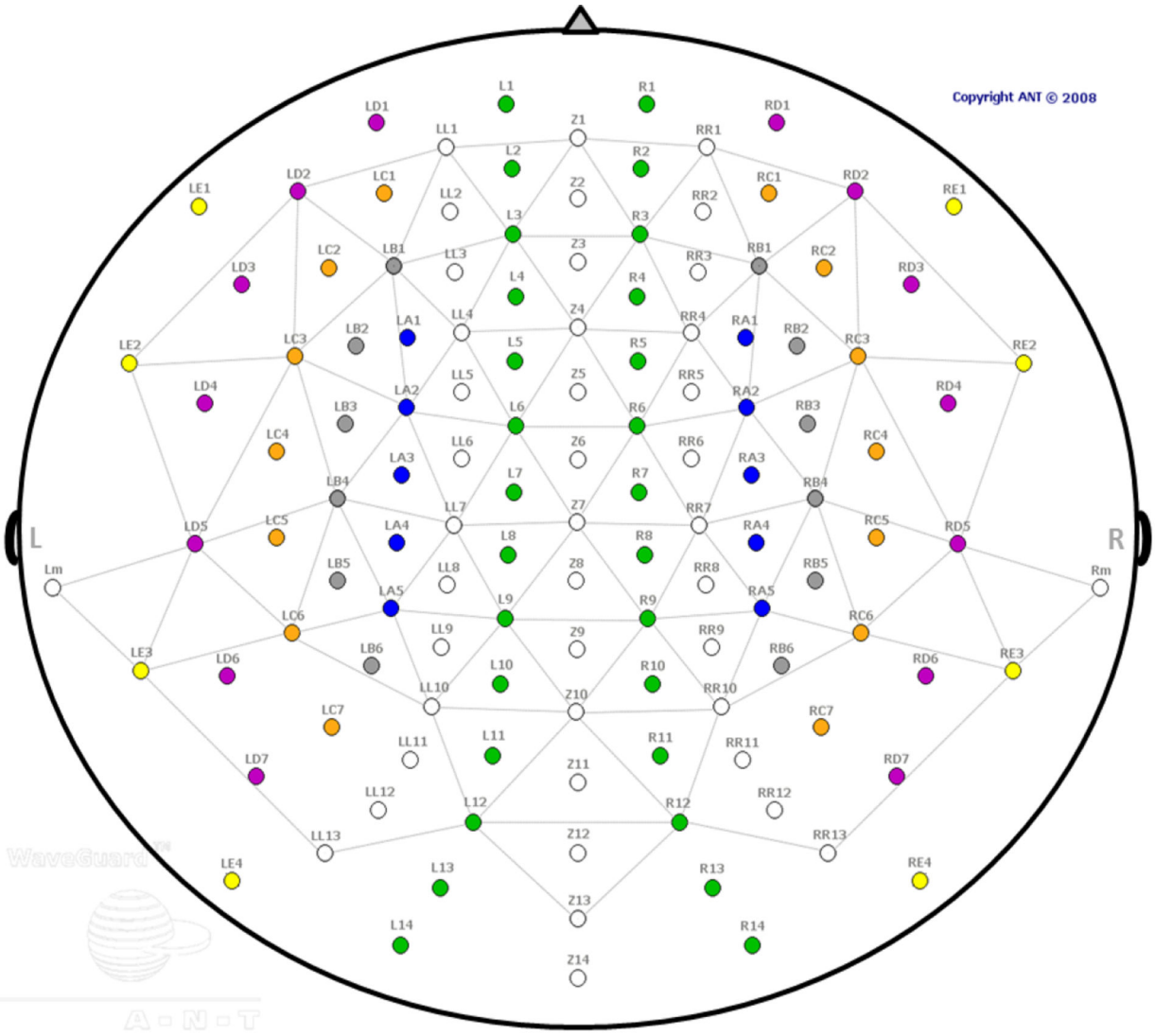

Figure 2. EEG sensor layout

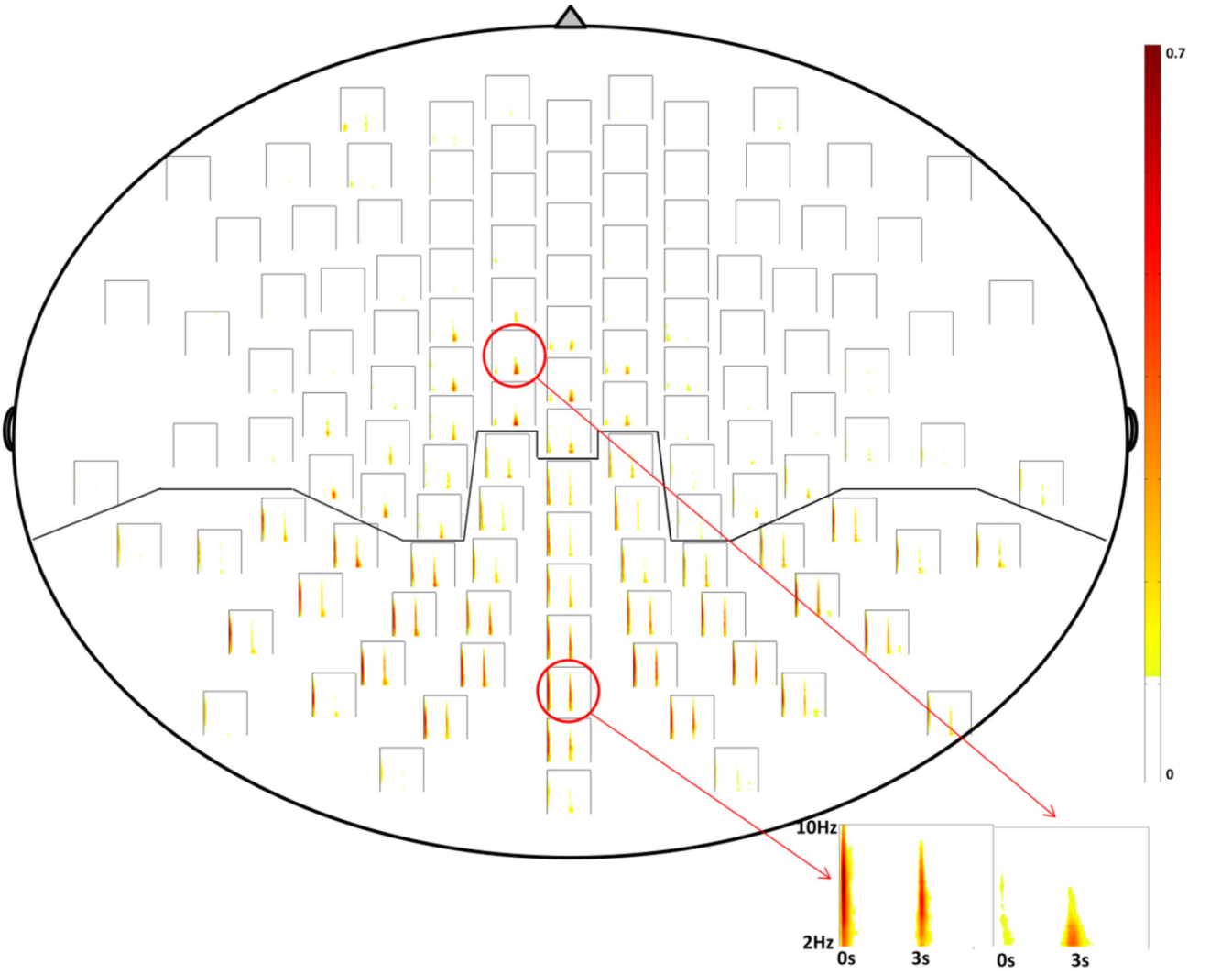

Figure 3. Grand average Matching Pursuit (MP) results demonstrating event-related synchronization (ERS)

The diagram is oriented as an "overhead" view of the scalp, with the nose at the top of the page and occiput at the bottom. Each plot within the diagram represents change in energy of EEG signal indexed by ERS of underlying cortical network; time is plotted on the x-axis, frequency (2–10 Hz) is plotted on the y-axis, and magnitude of ERS (relative to a baseline period) is indexed by intensity of color. ERS is seen from 0–1 sec (the first second following the onset of the *Prepare* stimulus) and 3–4 sec (the first second following the onset of the *Go* stimulus). The solid line shows the demarcation between parietal and frontal ROIs. Spectrograms representing the average of channels in each of the 4 ROIs are shown in greater detail in Fig. 4.

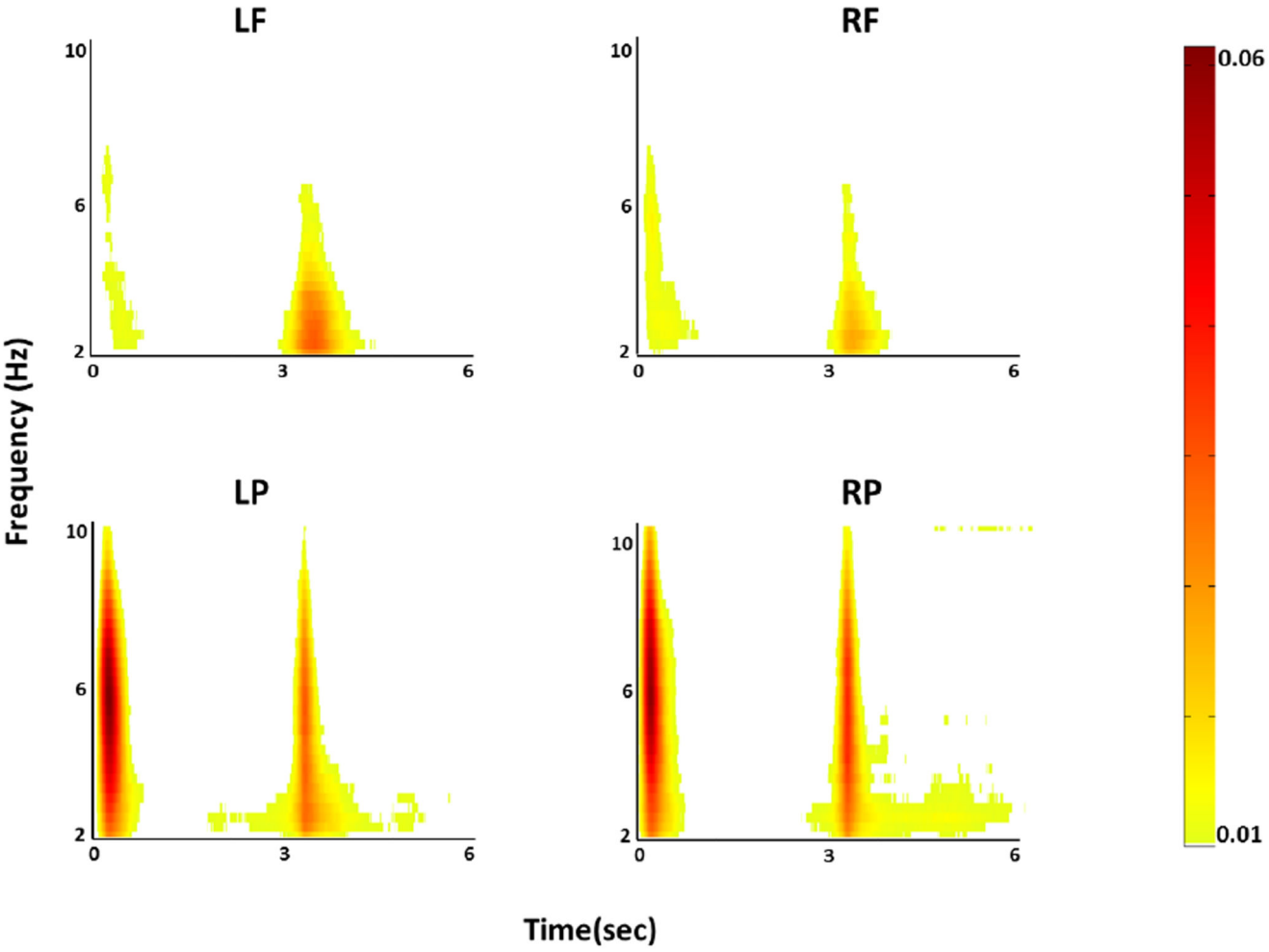

Figure 4. Average of ERS over ROIs for all subjects

Each time-frequency ERS plot (time: *x*-axis, frequency: *y*-axis) represents averaged increase in energy of all EEG signals of each ROI, for all subjects. ERS seen immediately following *Prepare* (0–1 sec) does not differ in magnitude between left and right hemispheres. Following *Go* (3–4 sec), ERS in the left frontal ROI was significantly greater in magnitude than ERS in the right frontal ROI. n.s. = non-significant. This asymmetry can also be seen in Figure 3.

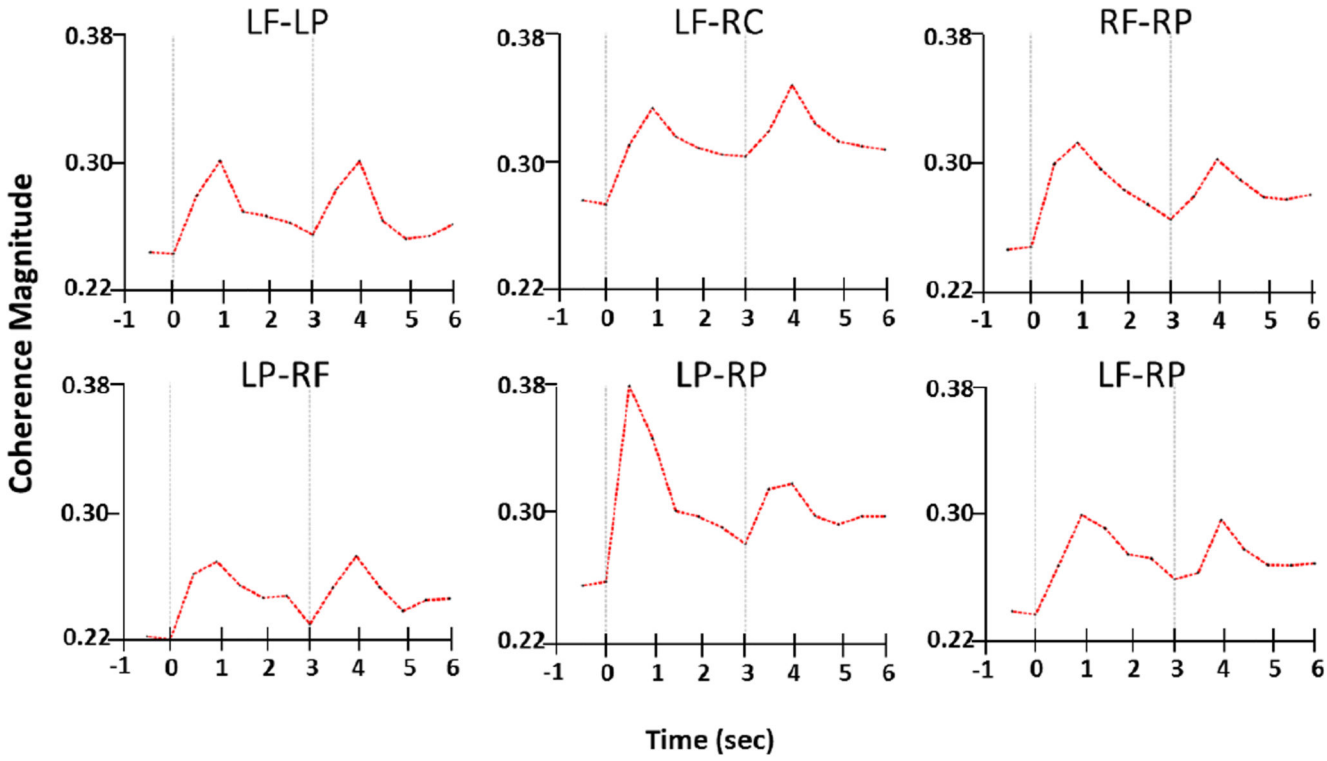

Figure 5. Averaged time courses of coherences between ROIs

Coherence results shows increases in functional connectivity following both *Prepare* and *Go* stimuli. The peak of the response to the *Prepare* stimulus is seen at one second, and the peak of the response to the *Go* stimulus is seen at four seconds due to lower time resolution (longer window) of the coherence function. Task-related coherence changes are seen in all ROI pairs.

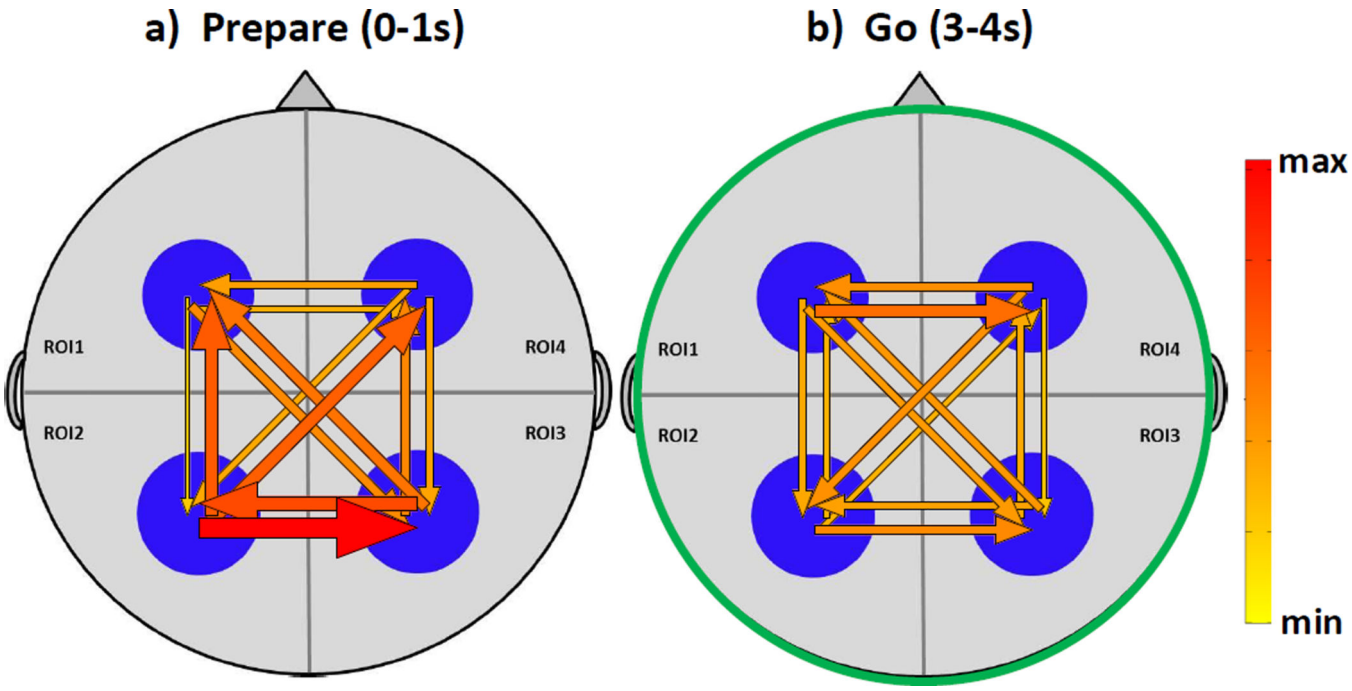

Figure 6. ERC results in the most active time segments (0–1s and 3–4s)

ERC demonstrates increases in directed propagations among regions of interest (ROI) for the two most active seconds of the experiment, using grand average data. Frame (a) represents event related causal interactions following onset of the *Prepare* stimulus, while (b) represents event-related causal propagations following onset of the *Go* stimulus, and correspond to the same timeframes used for coherence results shown in Fig. 5. The magnitude of ERC is greater at 0–1 sec (following *Prepare*) and 3–4 sec (following *Go*) than in other time bins.

Table 1

Table of p-values for comparisons of ERC measures.

PRAXIS	**Prepare (0–1s)**	**Go (3–4s)**
LC>RC	NS	p=1.2423e-005
LP>RP	NS	NS
LP>LC	p=2.9187e-006	NS
RP>RC	p=1.9087e-006	p=3.7506e-004
	0–1s vs 3–4s	
LP (0–1s > 3–4s)	p=5.045e-004	
RP (0–1s > 3–4s)	p=0.0096	
LC (3–4s > 0–1s)	p=3.5e-006	
RC	NS	